

Perturbative renormalization of moments of quark momentum, helicity and transversity distributions with overlap and Wilson fermions

Stefano Capitani

*Center for Theoretical Physics, Laboratory for Nuclear Science
Massachusetts Institute of Technology
77 Massachusetts Ave., Cambridge, MA 02139, USA*

E-mail: stefano@mitlns.mit.edu

Abstract

Using overlap as well as Wilson fermions, we have computed the one-loop renormalization factors of ten non-singlet operators which measure the third moment of quark momentum and helicity distributions (the lowest two having been computed in a previous paper), as well as the lowest three moments of the g_2 structure function and the lowest two non-trivial moments of the h_1 transversity structure function (plus the tensor charge). These factors are needed to extract physical observables from Monte Carlo simulations of the corresponding matrix elements.

An exact chiral symmetry is maintained in our calculations with overlap fermions, and its most important consequence here is that the operators measuring g_2 do not show any of the power-divergent mixings with operators of lower dimension which are present in the Wilson case. Many of our results for Wilson fermions are also new; for the remaining ones, we agree with the literature except in one case. The computations have been carried out using the symbolic language FORM, in a general covariant gauge, which turns out also to be useful in checking the gauge-invariance of the final results.

Keywords: Lattice QCD, Overlap-Dirac operator, Chirality, Structure functions, Lattice perturbation theory, Lattice renormalization.

PACS numbers: 11.15.-q, 11.15.Ha, 12.38.Gc, 13.60.Hb.

1 Introduction

Overlap fermions [1] have emerged in recent years as one of the most promising formulations for simulating on the lattice theories that possess an exact chiral symmetry. The overlap-Dirac operator proposed by Neuberger [2] is one of the solutions of the Ginsparg-Wilson relation [3]

$$\gamma_5 D + D \gamma_5 = a \frac{1}{\rho} D \gamma_5 D, \quad (1)$$

and allows the realization of an exact chiral symmetry also at non-zero lattice spacing [4] without giving up other important symmetries. Although simulations with the Neuberger operator look computationally demanding when compared with Wilson fermions, progress is under way in simulating overlap fermions and in improving the efficiencies of their simulation algorithms [5–8]. Results of some recent simulations show remarkable evidence of the signatures of the exact chiral symmetry. For example, Ref. [7] provides strong numerical evidence that the pion mass approaches zero in the limit $m_0 a \rightarrow 0$ without additive renormalization, in the two-dimensional Schwinger model, and progress is on the way for QCD; in Ref. [8] it is shown how the Gell-Mann-Oakes-Renner relation, which is a test of chiral symmetry at finite lattice spacing, is satisfied to better than 1% down to quark masses as small as $m_0 a = 0.006$. There is some confidence that overlap fermions will at the end turn out to be not too computationally demanding, and in any case one has to take into account all the advantages of having an exact chiral symmetry as well as the rapid progress in computer technology that is taking place these days.

In this paper we present the computation of the renormalization factors of many operators that measure moments of various structure functions, using overlap fermions. The operators that we consider include all three parton distributions that characterize the quarks in the nucleon and provide a complete description of quark momentum and spin at leading twist: the momentum distribution $q(x, Q^2)$, the helicity distribution $\Delta q(x, Q^2)$ and the transversity distribution $\delta q(x, Q^2)$. We also study the g_2 structure function, which receives contributions from twist-3 operators. For each one of these structure functions, we have included in our study all the moments that can be measured by operators for which all tensor indices are distinct. On the lattice with overlap fermions, all these operators are then multiplicatively renormalized.

One of the advantages of overlap fermions is that lattice renormalization does not induce any mixings with operators of the wrong chirality, as instead it happens with Wilson fermions. While this issue is of the utmost importance in lattice simulations concerning weak decays and quantities like the CP-violation parameter e'/ϵ [9], it is also relevant here for some of the operators that mea-

sure the g_2 structure function, which for Wilson fermions mix with coefficients diverging as $1/a$, while for overlap fermions they are multiplicatively renormalized (see Sect. 5). Another advantage of overlap fermions is the reduction of the number of independent renormalization factors in a given physical situation, as can be seen here with the operators measuring unpolarized and polarized structure functions which differ by a γ_5 matrix. Significant computational gains are achieved in the improvement of the action (which is not needed at all) and of the operators, as the construction of improved operators and the calculation of their renormalization constants is much simpler for overlap than for Wilson fermions (see Sect. 4). We think that this is really an important point for the operators considered in this paper, as the full $O(a)$ improvement of DIS operators with Wilson fermions involves a significant amount of careful and cumbersome calculations.

Among the other solutions of the Ginsparg-Wilson relation, a popular one is given by domain-wall fermions, where however the decoupling of the chiral modes is achieved only in the limit in which the number of points in the fifth additional dimension goes to infinity. One of the most attractive features of overlap fermions is that, on the contrary, chiral symmetry is fully preserved for any finite volume of the lattice. As the authors of Ref. [10] state, “in practical applications, it is our present experience that it is easier to control chiral symmetry violations with Neuberger’s operator”.

The renormalization with overlap fermions of the lowest two moments of the quark momentum and helicity distributions has been already carried out in Ref. [11], and we refer to that paper for the general framework and conventions, as well as for the Feynman rules of the overlap theory that we use here. We recall only that the explicit form of the overlap-Dirac operator is

$$D_N = \frac{1}{a}\rho \left[1 + \frac{X}{\sqrt{X^\dagger X}} \right], \quad (2)$$

where

$$X = D_W - \frac{1}{a}\rho, \quad (3)$$

with $0 < \rho < 2r$, in terms of the usual Wilson-Dirac operator

$$D_W = \frac{1}{2} \left[\gamma_\mu (\nabla_\mu^* + \nabla_\mu) - ar \nabla_\mu^* \nabla_\mu \right], \quad (4)$$

$$\nabla_\mu \psi(x) = \frac{1}{a} \left[U(x, \mu) \psi(x + a\hat{\mu}) - \psi(x) \right]. \quad (5)$$

Since the renormalization constants for many of the operators considered in this paper had not even been computed with Wilson fermions, we have calculated them for all the operators considered here with Wilson fermions too, and in this way we have also checked some old results in the literature, finding a discrepancy in one case.

This paper is organized as follows: in Sect. 2 we introduce the various operators of which we have computed the renormalization constants, in Sect. 3 their renormalization on the lattice is discussed and some details about the perturbative calculations are given, in Sect. 4 we discuss the advantages of using overlap over Wilson fermions with regard to the improvement, and in Sect. 5 we present the complete results. In the appendices we give the results for the quark self-energy, both for overlap and for Wilson fermions, and for the individual proper diagrams.

2 Moments of structure functions

We have considered in this paper the lowest moments of a few structure functions which give a complete description of quark momentum and spin at leading twist: the momentum distribution $q(x, Q^2)$, measured by the F_1 and F_2 unpolarized structure functions, the helicity distribution $\Delta q(x, Q^2)$, measured by the g_1 structure function, and the transversity distribution $\delta q(x, Q^2)$, measured by the h_1 structure function [12,13]. We have also considered the g_2 structure function [14], which measures the transverse spin, is chiral even and contains at leading order a twist-3 piece; it is one of the most accessible higher-twist quantities. The h_1 structure function is instead chiral odd and as such does not arise in inclusive DIS and can be measured instead in polarized Drell-Yan processes. For some more detailed discussions of deep inelastic scattering on the lattice, see Refs. [15–20,11] and references therein.

The moments of the various distributions are, for a given flavor ¹,

¹ We have chosen our conventions in such a way that there is a manifest symmetry between v_n and a_n . The operators corresponding to v_n and a_n have the same number of covariant derivatives, corresponding chiral properties, and the same renormalization constant for overlap fermions [11], as well as obviously in any continuum scheme. The same convention was also used in Ref. [11] and can be found for example in [21], but in other papers like e. g. [17,19] a_n has a correspondence with v_{n+1} .

In all operators considered here the subscript n equals the number of symmetrized Lorentz indices. This means that for the operators measuring d_n our convention is still the same as [17,19].

$$\begin{aligned}
2 \int_0^1 dx x^{n-1} F_1(x, Q^2) &= C_{1,n} \left(\frac{Q^2}{\mu^2}, g(\mu) \right) v_n(\mu) \\
\int_0^1 dx x^{n-2} F_2(x, Q^2) &= C_{2,n} \left(\frac{Q^2}{\mu^2}, g(\mu) \right) v_n(\mu) \\
2 \int_0^1 dx x^{n-1} g_1(x, Q^2) &= \frac{1}{2} E_{1,n} \left(\frac{Q^2}{\mu^2}, g(\mu) \right) a_n(\mu) \\
2 \int_0^1 dx x^{n-1} g_2(x, Q^2) &= \frac{1}{2} \frac{n-1}{n} \left(E_{2,n} \left(\frac{Q^2}{\mu^2}, g(\mu) \right) d_{n-1}(\mu) \right. \\
&\quad \left. - E_{1,n} \left(\frac{Q^2}{\mu^2}, g(\mu) \right) a_n(\mu) \right) \\
2 \int_0^1 dx x^{n-1} h_1(x, Q^2) &= \frac{1}{2} B_{1,n} \left(\frac{Q^2}{\mu^2}, g(\mu) \right) t_n(\mu),
\end{aligned} \tag{6}$$

where $C_{i,n}$, $E_{i,n}$ and $B_{1,n}$ denote the appropriate Wilson coefficients in the OPE expansions, which can be computed in continuum perturbation theory. The moments of the helicity and transversity distributions are given by the formulae

$$\begin{aligned}
a_{n+1} &= 2\Delta^{(n)}q, & \Delta^{(n)}q(\mu) &= \int_0^1 dx x^n \Delta q(x, \mu) \\
t_{n+1} &= 2\delta^{(n)}q, & \delta^{(n)}q(\mu) &= \int_0^1 dx x^n \delta q(x, \mu),
\end{aligned} \tag{7}$$

and the axial charge is $\Delta^{(0)}u - \Delta^{(0)}d = g_A = 1.26$.

The quark operators that correspond to the moments are ²

$$O_{\mu_1 \dots \mu_n} = \left(\frac{i}{2} \right)^{n-1} \bar{\psi} \gamma_{\mu_1} D_{\mu_2} \dots D_{\mu_n} \psi - \text{traces}$$

² We use $D = \vec{D} - \overleftarrow{D}$, with the following lattice discretizations:

$$\begin{aligned}
\vec{D}_\mu \psi(x) &= \frac{1}{2a} \left[U(x, \mu) \psi(x + a\hat{\mu}) - U^\dagger(x - a\hat{\mu}, \mu) \psi(x - a\hat{\mu}) \right] \\
\bar{\psi}(x) \overleftarrow{D}_\mu &= \frac{1}{2a} \left[\bar{\psi}(x + a\hat{\mu}) U^\dagger(x, \mu) - \bar{\psi}(x - a\hat{\mu}) U(x - a\hat{\mu}, \mu) \right].
\end{aligned} \tag{8}$$

$$\begin{aligned}
O_{\mu_1 \dots \mu_n}^5 &= \left(\frac{i}{2}\right)^{n-1} \bar{\psi} \gamma_{\mu_1} \gamma_5 D_{\mu_2} \cdots D_{\mu_n} \psi - \text{traces} \\
O_{\mu_1 \dots \mu_n}^h &= \left(\frac{i}{2}\right)^{n-2} \bar{\psi} \sigma_{\mu_1 \mu_2} \gamma_5 D_{\mu_3} \cdots D_{\mu_n} \psi - \text{traces}.
\end{aligned} \tag{9}$$

The matrix elements of the above operators on polarized quark states are

$$\begin{aligned}
\frac{1}{2} \sum_s \langle \vec{p}, \vec{s} | O_{\{\mu_1 \dots \mu_n\}} | \vec{p}, \vec{s} \rangle &= 2 v_n [p_{\mu_1} \cdots p_{\mu_n} - \text{traces}] \\
\langle \vec{p}, \vec{s} | O_{\{\mu_1 \dots \mu_n\}}^5 | \vec{p}, \vec{s} \rangle &= \frac{1}{n} a_n [s_{\{\mu_1 p_{\mu_2} \cdots p_{\mu_n}\}} + \cdots - \text{traces}] \\
\langle \vec{p}, \vec{s} | O_{[\mu_1 \{\mu_2\} \dots \mu_n]}^5 | \vec{p}, \vec{s} \rangle &= \frac{1}{n} d_{n-1} [s_{[\mu_1 p_{\{\mu_2\}} p_{\mu_3} \cdots p_{\mu_n}]} + \cdots - \text{traces}] \\
\langle \vec{p}, \vec{s} | O_{\mu_1 \{\mu_2 \dots \mu_n\}}^h | \vec{p}, \vec{s} \rangle &= \frac{1}{m_N} t_{n-1} [s_{[\mu_1 p_{\{\mu_2\}} p_{\mu_3} \cdots p_{\mu_n}]} + \cdots - \text{traces}],
\end{aligned} \tag{10}$$

where s_μ is the polarization vector of the nucleon, with $s^2 = -m_N^2$.

The moments of the various distributions can be studied from first principles by performing lattice Monte Carlo simulations of the above matrix elements, which determine then the various v_n , a_n , d_n and t_n quantities. These bare numbers need however to be renormalized. Under renormalization, the quark operators corresponding to momentum and helicity distributions mix in the flavor singlet case with operators that measure the corresponding gluon distributions. We consider in this paper only flavor non-singlet operators, so that the mixing with gluon operators is forbidden. The operators corresponding to the transversity distribution however do not have any gluon mixing even in the flavor-singlet case, as there is no gluonic transversity at leading twist, i. e. no chiral-odd gluon operator can be constructed.

In a previous paper we have calculated the renormalization factors of a few operators which measure v_2 , v_3 , a_2 and a_3 [11]; here we compute the renormalization constants of the operators

$$O_{v_4,d} = \bar{\psi} \gamma_{\{4} D_1 D_2 D_3 \} \psi \tag{11}$$

$$\begin{aligned}
O_{v_4,e} &= \bar{\psi} \gamma_{\{4} D_4 D_1 D_1 \} \psi + \bar{\psi} \gamma_{\{3} D_3 D_2 D_2 \} \psi \\
&\quad - \bar{\psi} \gamma_{\{4} D_4 D_2 D_2 \} \psi - \bar{\psi} \gamma_{\{3} D_3 D_1 D_1 \} \psi,
\end{aligned} \tag{12}$$

which measure the third moment of the quark momentum distribution, and

$$O_{a_4,d} = \bar{\psi} \gamma_{\{4} \gamma_5 D_1 D_2 D_3 \} \psi \tag{13}$$

$$\begin{aligned}
O_{a_4,e} &= \bar{\psi} \gamma_{\{4} \gamma_5 D_4 D_1 D_1 \} \psi + \bar{\psi} \gamma_{\{3} \gamma_5 D_3 D_2 D_2 \} \psi \\
&\quad - \bar{\psi} \gamma_{\{4} \gamma_5 D_4 D_2 D_2 \} \psi - \bar{\psi} \gamma_{\{3} \gamma_5 D_3 D_1 D_1 \} \psi,
\end{aligned} \tag{14}$$

which measure the third moment of the g_1 quark helicity distribution. Together with the computations in Ref. [11], they complete the calculation of the renormalization factors of the lowest three moments of these distributions; each continuum operator has been considered twice on the lattice by choosing its indices in two different ways, corresponding to two different representations of the hypercubic group for the same moment, which renormalize independently on the lattice.

We have computed also the renormalization constants of the operators

$$O_{d_1} = \bar{\psi}\gamma_{[4}\gamma_5 D_{1]}\psi \quad (15)$$

$$O_{d_2} = \bar{\psi}\gamma_{[4}\gamma_5 D_{\{1\}}D_{2\}}\psi \quad (16)$$

$$= \frac{1}{2} \left(\bar{\psi}\gamma_4\gamma_5 D_1 D_2 \psi + \bar{\psi}\gamma_4\gamma_5 D_2 D_1 \psi - \bar{\psi}\gamma_1\gamma_5 D_4 D_2 \psi - \bar{\psi}\gamma_1\gamma_5 D_2 D_4 \psi \right)$$

$$O_{d_3} = \bar{\psi}\gamma_{[4}\gamma_5 D_{\{1\}}D_{2\}}D_{3\}}\psi \quad (17)$$

$$= \frac{1}{6} \left(\bar{\psi}\gamma_4\gamma_5 D_1 D_2 D_3 \psi + \bar{\psi}\gamma_4\gamma_5 D_1 D_3 D_2 \psi + \bar{\psi}\gamma_4\gamma_5 D_2 D_1 D_3 \psi \right. \\ \left. + \bar{\psi}\gamma_4\gamma_5 D_2 D_3 D_1 \psi + \bar{\psi}\gamma_4\gamma_5 D_3 D_1 D_2 \psi + \bar{\psi}\gamma_4\gamma_5 D_3 D_2 D_1 \psi \right. \\ \left. - \bar{\psi}\gamma_1\gamma_5 D_4 D_2 D_3 \psi - \bar{\psi}\gamma_1\gamma_5 D_4 D_3 D_2 \psi - \bar{\psi}\gamma_1\gamma_5 D_2 D_4 D_3 \psi \right. \\ \left. - \bar{\psi}\gamma_1\gamma_5 D_2 D_3 D_4 \psi - \bar{\psi}\gamma_1\gamma_5 D_3 D_4 D_2 \psi - \bar{\psi}\gamma_1\gamma_5 D_3 D_2 D_4 \psi \right),$$

which taken together with O_{a_2} , O_{a_3} and O_{a_4} determine the lowest three moments of the g_2 structure function in Eq. (6). In the Wilson case each one of the O_{d_n} operators,

$$\bar{\psi}\gamma_{[\sigma}\gamma_5 D_{\{\mu_1\}}D_{\mu_2} \cdots D_{\mu_n\}}\psi, \quad (18)$$

mixes, due to the breaking of chirality, with a lower-dimensional operator which in the continuum OPE has a mass coefficient [14],

$$m_q \bar{\psi}\gamma_{[\sigma}\gamma_5 \gamma_{\{\mu_1\}}D_{\mu_2} \cdots D_{\mu_n\}}\psi, \quad (19)$$

but on the lattice this mass becomes a $1/a$ divergent coefficient. This mixing is forbidden in the overlap case, and the O_{d_n} operators are multiplicatively renormalized. Thus the overlap makes a complete perturbative renormalization of these operators possible.

Regarding the transversity distribution h_1 , we have considered the twist-two operators that measure the tensor charge and the lowest two non-trivial moments,

$$O_{t_1} = \bar{\psi}\sigma_{41}\gamma_5\psi \quad (20)$$

$$O_{t_2} = \bar{\psi} \sigma_{4\{1\gamma_5 D_2\}} \psi \quad (21)$$

$$O_{t_3} = \bar{\psi} \sigma_{4\{1\gamma_5 D_2 D_3\}} \psi. \quad (22)$$

The moments of the various distributions shown above are all the ones that can be associated with an operator which has all the indices different from each other. There is then no mixing due to the breaking of the Lorentz group to the hypercubic group. In fact, all the above operators are multiplicatively renormalized in the overlap case; this is true also for the particular combinations in $O_{v_4,e}$ and $O_{a_4,e}$ in which some of the indices are equal. The O_{d_n} operators are not multiplicatively renormalized when using Wilson fermions, but their mixings are in this case due only to the breaking of chiral symmetry.

All operators measuring higher moments of the above distributions necessarily have at least two equal indices. In fact, the operators which would be next in the ladder of moments have five Lorentz indices and therefore two of them have to be equal:

$$\begin{aligned} O_{v_5} &= \bar{\psi} \gamma_{\{4} D_1 D_1 D_2 D_3\} \psi \\ O_{a_5} &= \bar{\psi} \gamma_{\{4} \gamma_5 D_1 D_1 D_2 D_3\} \psi \\ O_{d_4} &= \bar{\psi} \gamma_{\{4} \gamma_5 D_{\{1\}} D_1 D_2 D_3\} \psi \\ O_{t_4} &= \bar{\psi} \sigma_{4\{1\gamma_5 D_1 D_2 D_3\}} \psi. \end{aligned} \quad (23)$$

This leaves open the possibility of mixing with same-dimension or (more catastrophic) lower-dimension operators. We do not address here this problem, which is left for further studies.

3 Perturbative renormalization

The raw numbers extracted from Monte Carlo simulations need to be renormalized to physical continuum quantities. The connection is given by

$$\langle O_i^{\text{cont}} \rangle = \sum_j \left(\delta_{ij} - \frac{g_0^2}{16\pi^2} (R_{ij}^{\text{lat}} - R_{ij}^{\text{cont}}) \right) \cdot \langle O_j^{\text{lat}} \rangle, \quad (24)$$

where

$$\langle O_i^{\text{cont,lat}} \rangle = \sum_j \left(\delta_{ij} + \frac{g_0^2}{16\pi^2} R_{ij}^{\text{cont,lat}} \right) \cdot \langle O_j^{\text{tree}} \rangle \quad (25)$$

are the continuum and lattice 1-loop expressions respectively, and the tree-level matrix element is the same in both cases. Their difference $\Delta R_{ij} = R_{ij}^{\text{lat}} - R_{ij}^{\text{cont}}$ enters then in the gauge-invariant renormalization factors

$$Z_{ij}(a\mu, g_0) = \delta_{ij} - \frac{g_0^2}{16\pi^2} \Delta R_{ij}(a\mu), \quad (26)$$

which renormalize the results of Monte Carlo simulations to a continuum scheme.

We choose as continuum scheme the $\overline{\text{MS}}$ scheme, since commonly the Wilson coefficients are computed in this scheme. On the lattice the renormalization condition is that the 1-loop amputated matrix elements at a certain reference scale μ are equal to the corresponding bare tree-level quantities. For lattice matrix elements of multiplicatively renormalized operators computed between one-quark states, this condition reads

$$\begin{aligned} \langle p|O^{\text{lat}}(\mu)|p\rangle\Big|_{p^2=\mu^2} &= Z_O(a\mu, g_0) \cdot Z_\psi^{-1}(a\mu, g_0) \cdot \langle p|O^{(0)}(a)|p\rangle\Big|_{p^2=\mu^2}^{1\text{-loop}} \\ &= \langle p|O^{(0)}(a)|p\rangle\Big|_{p^2=\mu^2}^{\text{tree}}, \end{aligned} \quad (27)$$

where Z_ψ is the wave-function renormalization, computed from the quark self-energy.

The 1-loop lattice matrix element of a logarithmically divergent operator O has the form

$$\begin{aligned} \langle p|O^{(0)}(a)|p\rangle\Big|^{1\text{-loop}} &= \langle p|O^{(0)}(a)|p\rangle\Big|_{p^2=\mu^2}^{\text{tree}} \times \\ &\quad \left(1 + \frac{g_0^2}{16\pi^2} C_F (\gamma_O \log a^2 p^2 + V_O + T_O + 2S)\right), \end{aligned} \quad (28)$$

where V_O is the finite contribution of the vertex and sails diagrams (a, b and c in Fig. 1), T_O refers to the tadpole arising from the operator (d in Fig. 1), and S is the finite contribution (proportional to $i\not{p}$) of the quark self-energy of one leg, including the leg tadpole (e and g, or f and h, in Fig. 1). We have also that $C_F = \frac{N_c^2 - 1}{2N_c}$ for the $SU(N_c)$ gauge group. The Z_O factor for the operator O is then given by

$$Z_O(a\mu, g_0) = 1 - \frac{g_0^2}{16\pi^2} C_F \left(\gamma_O \log a^2 \mu^2 + B_O\right), \quad (29)$$

with

$$B_O = V_O + T_O + S. \quad (30)$$

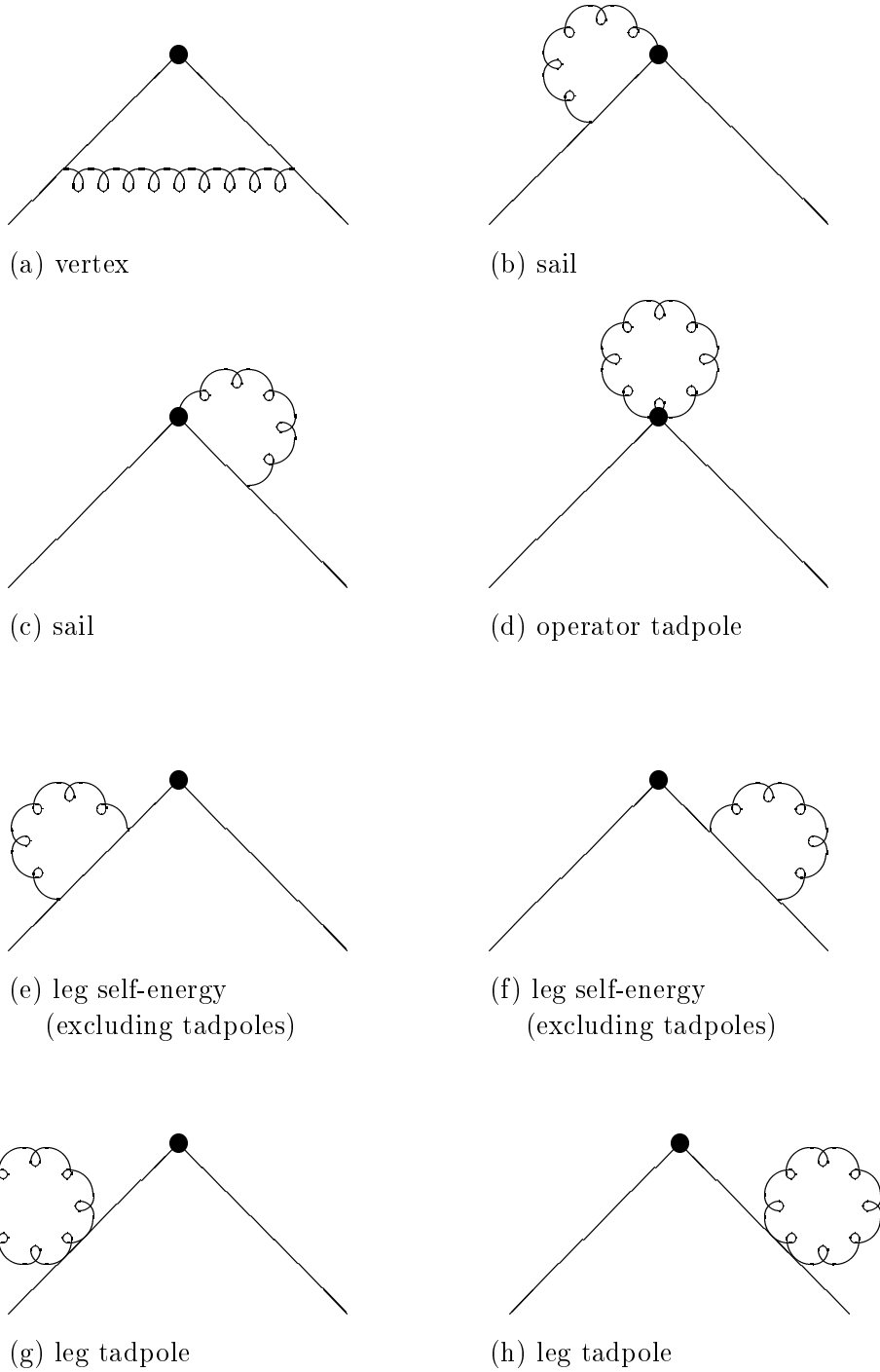


Fig. 1. The graphs contributing to the 1-loop renormalization factors of the matrix elements $\langle p|O|p\rangle$. The operator insertion is indicated by a circle.

We will call “proper” contributions the ones that do not include the self-energy diagrams. They correspond to the diagrams a-d in Fig. 1.

We have used computer programs to carry out the calculations of the Feynman diagrams, given their complexities and the huge number of terms that are present in some cases. They utilize an ensemble of routines written in the symbolic manipulation language FORM, and are able to do the analytic calculations; Fortran codes subsequently perform the numerical integrations. These routines are an extension of the ones used to do calculations with the Wilson action in various occasions [19,22] and to compute the first two moments of the momentum and helicity distributions with overlap fermions [11]. Some more details can be found in Ref. [11].

We would like to stress that one of the major checks of our calculations, which are all done in a general covariant gauge ³, is the cancellation of the gauge-dependent terms proportional to $(1 - \alpha)$ in the final numbers that connect the lattice to the $\overline{\text{MS}}$ scheme, as in Eq. (26). Another significant check with overlap fermions is that the operators $O_{v_4,d}$ and $O_{a_4,d}$ have the same Z well within numerical integration errors, as well as $O_{v_4,e}$ and $O_{a_4,e}$, as expected from chiral symmetry. Furthermore, we verified that there is no $1/a$ mixing term in the 1-loop expressions of the operators O_{d_1} , O_{d_2} and O_{d_3} , contrary to what happens in the Wilson case.

The computations of the integrals for the operators $O_{v_4,e}$, $O_{a_4,e}$ and O_{d_3} have been the most demanding. We had to split the FORM outputs in several pieces as otherwise the Fortran programs would refuse to compile them. The running time for the computation of the integrals on a 60^4 grid has been in these cases of the order of 500 hours on a 500 MHz CPU.

4 Improvement: overlap versus Wilson fermions

To highlight the advantages of overlap fermions relative to Wilson fermions, we summarize the differences in $O(a)$ improvement using each method.

Although the overlap-Dirac action possesses an exact chiral symmetry and has no $O(a)$ terms, matrix elements of operators do have order a corrections and therefore they need to be improved. The operators considered in this paper,

³ The gluon propagator that we use is

$$G_{\mu\nu}(k) = \frac{1}{4 \sum_{\rho} \sin^2 \frac{k_{\rho}}{2}} \left(\delta_{\mu\nu} - (1 - \alpha) \frac{4 \sin \frac{k_{\mu}}{2} \sin \frac{k_{\nu}}{2}}{4 \sum_{\lambda} \sin^2 \frac{k_{\lambda}}{2}} \right). \quad (31)$$

which are all of the form $O = \bar{\psi}\tilde{O}\psi$, are made free of $O(a)$ corrections by taking [23]

$$O^{\text{imp}} = \bar{\psi}\left(1 - \frac{1}{2\rho}aD_N\right)\tilde{O}\left(1 - \frac{1}{2\rho}aD_N\right)\psi. \quad (32)$$

Thus, in the overlap formulation, by rotating the spinors as in Eq. (32), operators are freed of $O(a)$ corrections. In Ref. [22] it has been shown that this recipe improves the operators to all orders of perturbation theory. Thus, full $O(a)$ improvement is achieved without tuning any coefficients. Furthermore, the renormalization constants for the improved and unimproved operators are the same, so there is no need to do additional calculations, which are generally cumbersome, to compute the renormalization factors in the improved theory. What happens is that in 1-loop amplitudes a factor D_N can combine with a quark propagator, but since it has an a in front and (contrary to the Wilson case) there is no $1/a$ piece in the propagator, as additive mass renormalization is forbidden by chiral symmetry, the contribution of D_N to the renormalization factors is zero [24]. Thus, improved Monte Carlo simulations are performed with the operator (32), nevertheless the renormalization of this operator is equal to that of the corresponding unimproved operator.

For Wilson fermions, instead, the improvement of operators looks more complicated and troublesome. First of all, one has to find out a complete basis which includes all operators which are one-dimension higher than the original one and have the same symmetries. Then, to get the improved renormalization factors, which are different from the unimproved ones, one has to compute the 1-loop matrix elements of each one of those operators. Lastly, one has to determine somehow the values of the coefficients in front of the operator counterterms, and this appears to be a highly non-trivial task.

Let us consider, for example, the first moment of the quark momentum distribution, $O_{v_2} = \bar{\psi}\gamma_{\{\mu}D_{\nu\}}\psi$. The improvement counterterms are two dimension-five operators [22], and one basis for the improvement is given by

$$\bar{\psi}\gamma_{\{\mu}D_{\nu\}}\psi - \frac{1}{4}aic_1(g_0^2)\sum_{\lambda}\bar{\psi}\sigma_{\lambda\{\mu}[D_{\nu\}},D_{\lambda}]\psi - \frac{1}{4}ac_2(g_0^2)\bar{\psi}\{D_{\mu},D_{\nu}\}\psi. \quad (33)$$

The operator is fully $O(a)$ improved only for some particular values of the coefficients $c_1(g_0^2) = 1 + g_0^2c_1^{(1)} + O(g_0^4)$ and $c_2(g_0^2) = 1 + g_0^2c_2^{(1)} + O(g_0^4)$. However, presently one knows only a relation between the two coefficients [22], and thus one of them remains unknown. Although one could determine all coefficients using some Ward Identities or physical conditions, this involves more effort than with overlap fermions. In addition, the coefficients are different for different orders in perturbation theory, and the basis itself is different for

each operator to be improved. It is reasonable to expect that operators which contain more covariant derivatives will have larger improvement bases, and thus many more coefficients to be determined, besides computing the 1-loop matrix elements for each of the operator counterterms. Presumably already implementing the improvement for the second moment operators with Wilson fermions will turn out to be a daunting task. This means that in most cases it will be difficult to go beyond tree-level improvement for the structure function operators in the Wilson case.

In addition to improving operators, one should also note that Wilson fermions need corrections to their action (the Sheikholeslami-Wohlert term), while the overlap action is already $O(a)$ improved. However, this is less of a complication than the improvement of the operators.

Thus, for all these reasons, from the perspective of renormalization, mixing, and improvement, overlap fermions offer compelling advantages relative to Wilson fermions.

5 Results

We give in this section the results for the renormalization factors of every operator considered in this paper, both for the overlap and the Wilson action, for $r = 1$.

In the overlap case, we have explicitly verified that the renormalization constants of $O_{a_4,d}$ and $O_{a_4,e}$ are equal to the ones of $O_{v_4,d}$ and $O_{v_4,e}$ respectively, which are given below. This is a consequence of the exact chiral symmetry which the overlap theory possesses. Another important gain coming from chiral symmetry is that the operators O_{d_1} , O_{d_2} and O_{d_3} are multiplicatively renormalized, while for Wilson fermions the breaking of chiral symmetry causes a mixing with operators of lower dimensions, with the mixing coefficients going to infinity in the continuum limit.

5.1 Overlap fermions

We first consider the 1-loop contributions of the proper diagrams (a-d in Fig. 1), which are

$$O_{v_4,d}^{\text{proper}} = \frac{g_0^2}{16\pi^2} C_F \left[\left(\frac{127}{30} + (1 - \alpha) \right) \log a^2 p^2 \right]$$

ρ	$V_{v_4,d}^{\alpha=1}$	$V_{v_4,e}^{\alpha=1}$	$V_{d_1}^{\alpha=1}$	$V_{d_2}^{\alpha=1}$	$V_{d_3}^{\alpha=1}$	$V_{t_1}^{\alpha=1}$	$V_{t_2}^{\alpha=1}$	$V_{t_3}^{\alpha=1}$
0.2	-9.61600	-7.98774	52.66717	45.13633	41.92810	5.38049	-4.02560	-7.79945
0.3	-9.46984	-7.84341	33.37857	26.64726	23.65026	5.19029	-4.00839	-7.70244
0.4	-9.34521	-7.72067	24.03566	17.76727	14.91522	5.03112	-3.99077	-7.61751
0.5	-9.23484	-7.61223	18.60963	12.65715	9.91543	4.89210	-3.97274	-7.54054
0.6	-9.13474	-7.51412	15.11256	9.39617	6.74341	4.76733	-3.95427	-7.46925
0.7	-9.04244	-7.42384	12.70136	7.17180	4.59344	4.65325	-3.93535	-7.40221
0.8	-8.95626	-7.33973	10.95882	5.58297	3.06844	4.54744	-3.91595	-7.33847
0.9	-8.87501	-7.26060	9.65553	4.40974	1.95101	4.44823	-3.89606	-7.27733
1.0	-8.79780	-7.18557	8.65526	3.52185	1.11258	4.35437	-3.87564	-7.21828
1.1	-8.72396	-7.11394	7.87218	2.83746	0.47256	4.26491	-3.85467	-7.16091
1.2	-8.65295	-7.04517	7.24967	2.30276	-0.02200	4.17912	-3.83313	-7.10491
1.3	-8.58433	-6.97884	6.74895	1.88097	-0.40718	4.09639	-3.81099	-7.05001
1.4	-8.51774	-6.91457	6.34259	1.54618	-0.70839	4.01623	-3.78821	-6.99600
1.5	-8.45289	-6.85207	6.01069	1.27965	-0.94394	3.93824	-3.76477	-6.94269
1.6	-8.38952	-6.79107	5.73851	1.06752	-1.12735	3.86206	-3.74064	-6.88993
1.7	-8.32742	-6.73135	5.51486	0.89934	-1.26882	3.78741	-3.71578	-6.83758
1.8	-8.26640	-6.67272	5.33115	0.76710	-1.37612	3.71403	-3.69017	-6.78553

Table 1

The Feynman-gauge constants $V_O^{\alpha=1}$ for the momentum, helicity and transversity operators considered in this work, in the overlap theory. Note that in this case $V_{a_4,d}^{\alpha=1} = V_{v_4,d}^{\alpha=1}$ and $V_{a_4,e}^{\alpha=1} = V_{v_4,e}^{\alpha=1}$.

$$\begin{aligned}
& +V_{v_4,d}^{\alpha=1} - (1 - \alpha) 7.553824 + T_{v_4,d} \Big] O_{v_4,d}^{\text{tree}}, \\
O_{v_4,e}^{\text{proper}} &= \frac{g_0^2}{16\pi^2} C_F \left[\left(\frac{127}{30} + (1 - \alpha) \right) \log a^2 p^2 \right. \\
& \left. +V_{v_4,e}^{\alpha=1} - (1 - \alpha) 8.024764 + T_{v_4,e} \right] O_{v_4,e}^{\text{tree}}, \\
O_{d_1}^{\text{proper}} &= \frac{g_0^2}{16\pi^2} C_F \left[-\alpha \log a^2 p^2 + V_{d_1}^{\alpha=1} - (1 - \alpha) 7.850272 + T_{d_1} \right] O_{d_1}^{\text{tree}}, \\
O_{d_2}^{\text{proper}} &= \frac{g_0^2}{16\pi^2} C_F \left[\left(\frac{1}{6} + (1 - \alpha) \right) \log a^2 p^2 \right.
\end{aligned} \tag{34}$$

operator	operator tadpole
$O_{v_4,d}, O_{a_4,d}$	$T_{v_4,d} = T_{a_4,d} = 16\pi^2 \left(-\frac{3}{2}Z_0 + (1-\alpha) \left(-\frac{1}{24}Z_0 - \frac{1}{4}Z_1 + \frac{1}{16} \right) \right)$
$O_{v_4,e}, O_{a_4,e}$	$T_{v_4,e} = T_{a_4,e} = 16\pi^2 \left(-\frac{5}{2}Z_0 - \frac{1}{3}Z_1 + \frac{1}{6} + (1-\alpha) \left(\frac{9}{8}Z_0 + Z_1 - \frac{1}{4} \right) \right)$
O_{d_1}	$T_{d_1} = 16\pi^2 \left(-\frac{1}{2}Z_0 + (1-\alpha) \frac{1}{8}Z_0 \right)$
O_{d_2}	$T_{d_2} = 16\pi^2 \left(-Z_0 + (1-\alpha) \frac{1}{6}Z_0 \right)$
O_{d_3}	$T_{d_3} = 16\pi^2 \left(-\frac{3}{2}Z_0 + (1-\alpha) \left(-\frac{1}{24}Z_0 - \frac{1}{4}Z_1 + \frac{1}{16} \right) \right)$
O_{t_1}	$T_{t_1} = 0$
O_{t_2}	$T_{t_2} = 16\pi^2 \left(-\frac{1}{2}Z_0 + (1-\alpha) \frac{1}{8}Z_0 \right)$
O_{t_3}	$T_{t_3} = 16\pi^2 \left(-Z_0 + (1-\alpha) \frac{1}{6}Z_0 \right)$

Table 2

The operator tadpoles for the various operators, where $Z_0 = 0.154933390231 \dots$ and $Z_1 = 0.107781313540 \dots$.

$$\begin{aligned}
O_{d_3}^{\text{proper}} &= \frac{g_0^2}{16\pi^2} C_F \left[\left(\frac{17}{18} + (1-\alpha) \right) \log a^2 p^2 \right. \\
&\quad \left. + V_{d_2}^{\alpha=1} - (1-\alpha) 8.369693 + T_{d_2} \right] O_{d_2}^{\text{tree}} \\
&\quad \left. + V_{d_3}^{\alpha=1} - (1-\alpha) 8.553824 + T_{d_3} \right] O_{d_3}^{\text{tree}} \\
O_{t_1}^{\text{proper}} &= \frac{g_0^2}{16\pi^2} C_F \left[(1-\alpha) \log a^2 p^2 \right. \\
&\quad \left. + V_{t_1}^{\alpha=1} - (1-\alpha) 3.792010 + T_{t_1} \right] O_{t_1}^{\text{tree}}
\end{aligned}$$

$$\begin{aligned}
O_{t_2}^{\text{proper}} &= \frac{g_0^2}{16\pi^2} C_F \left[\left(2 + (1 - \alpha) \right) \log a^2 p^2 \right. \\
&\quad \left. + V_{t_2}^{\alpha=1} - (1 - \alpha) 6.350272 + T_{t_2} \right] O_{t_2}^{\text{tree}} \\
O_{t_3}^{\text{proper}} &= \frac{g_0^2}{16\pi^2} C_F \left[\left(\frac{10}{3} + (1 - \alpha) \right) \log a^2 p^2 \right. \\
&\quad \left. + V_{t_3}^{\alpha=1} - (1 - \alpha) 7.036360 + T_{t_3} \right] O_{t_3}^{\text{tree}}.
\end{aligned}$$

The Feynman gauge results $V_O^{\alpha=1}$ for the contributions of the sails and vertices, V_O , are tabulated in Table 1 for several values of the parameter ρ . They are also given separately for each diagram in Appendix B (for $\rho = 1$). The remaining parts proportional to $(1 - \alpha)$ are instead independent of ρ , and as their analytic expressions are very complicated functions of ρ containing thousands of terms, the numerical cancellation of this dependence is a highly non-trivial check of our computations. Furthermore, the parts proportional to $(1 - \alpha)$ have also the same value as with the Wilson action [11]. In fact they depend only on the gluonic action chosen.

The result for the tensor charge $O_{t_1} = \bar{\psi} \sigma_{\mu\nu} \gamma_5 \psi$ turns out to be equal to the result for the standard tensor current $\bar{\psi} \sigma_{\mu\nu} \psi$, which has been calculated in Ref. [24] in Feynman gauge and in Ref. [9] in a general covariant gauge. For Wilson fermions, the renormalization of O_{t_1} can be found in [22].

The results for the remaining proper diagram, the operator tadpole T_O (diagram d in Fig. 1), are shown in Table 2. To compute the renormalization factors, one finally adds to the proper diagrams the 1-loop amplitudes of the self-energy and tadpole of one leg which are proportional to $i\not{p}$. Their values are given in Appendix A. Putting everything together, we get the expressions of the renormalized operators on the lattice for overlap fermions, which for $\rho = 1$ are:

$$\begin{aligned}
\widehat{O}_{v_4,d} &= \left[1 - \frac{g_0^2}{16\pi^2} C_F \left(\frac{157}{30} \log a^2 \mu^2 - 83.12758 + \frac{11}{6}(1 - \alpha) \right) \right] O_{v_4,d}^{\text{tree}} \\
\widehat{O}_{v_4,e} &= \left[1 - \frac{g_0^2}{16\pi^2} C_F \left(\frac{157}{30} \log a^2 \mu^2 - 85.33588 + \frac{11}{6}(1 - \alpha) \right) \right] O_{v_4,e}^{\text{tree}} \\
\widehat{O}_{d_1} &= \left[1 + \frac{g_0^2}{16\pi^2} C_F \cdot 41.20842 \right] O_{d_1}^{\text{tree}} \\
\widehat{O}_{d_2} &= \left[1 - \frac{g_0^2}{16\pi^2} C_F \left(\frac{7}{6} \log a^2 \mu^2 - 58.57488 + \frac{1}{2}(1 - \alpha) \right) \right] O_{d_2}^{\text{tree}} \\
\widehat{O}_{d_3} &= \left[1 - \frac{g_0^2}{16\pi^2} C_F \left(\frac{35}{18} \log a^2 \mu^2 - 73.21719 + \frac{5}{6}(1 - \alpha) \right) \right] O_{d_3}^{\text{tree}}
\end{aligned} \tag{35}$$

$$\begin{aligned}
\hat{O}_{t_1} &= \left[1 - \frac{g_0^2}{16\pi^2} C_F \left(\log a^2 \mu^2 - 33.27626 + (1 - \alpha) \right) \right] O_{t_1}^{\text{tree}} \\
\hat{O}_{t_2} &= \left[1 - \frac{g_0^2}{16\pi^2} C_F \left(3 \log a^2 \mu^2 - 53.73932 + \frac{3}{2}(1 - \alpha) \right) \right] O_{t_2}^{\text{tree}} \\
\hat{O}_{t_3} &= \left[1 - \frac{g_0^2}{16\pi^2} C_F \left(\frac{13}{3} \log a^2 \mu^2 - 69.31500 + \frac{11}{6}(1 - \alpha) \right) \right] O_{t_3}^{\text{tree}}.
\end{aligned}$$

We see that in the overlap case the operators O_{d_1} , O_{d_2} and O_{d_3} are multiplicatively renormalized (contrary to what happens with Wilson fermions, see below).

Another check of our calculations is that the transversity operators, which apart from the trivial tensor charge have never been computed before on the lattice, agree with the 1-loop anomalous dimension formula [13]

$$\gamma_{t_n} = 1 + 4 \sum_{j=2}^n \frac{1}{j}, \quad (36)$$

which also implies that the anomalous dimensions are positive and for any given moment greater than the ones of the corresponding moments of F_1 , F_2 and g_1 .

To complete the connection with the continuum physics as in Eq. (24), we need also the 1-loop results for the same matrix elements in the continuum $\overline{\text{MS}}$ scheme, which are given by

$$\begin{aligned}
\hat{O}_{v_4}^{\overline{\text{MS}}} &= \left[1 - \frac{g_0^2}{16\pi^2} C_F \left(\frac{157}{30} \log a^2 \mu^2 - \frac{2216}{225} + \frac{11}{6}(1 - \alpha) \right) \right] O_{v_4}^{\text{tree}} \\
\hat{O}_{a_4}^{\overline{\text{MS}}} &= \left[1 - \frac{g_0^2}{16\pi^2} C_F \left(\frac{157}{30} \log a^2 \mu^2 - \frac{2216}{225} + \frac{11}{6}(1 - \alpha) \right) \right] O_{a_4}^{\text{tree}} \\
\hat{O}_{d_1}^{\overline{\text{MS}}} &= O_{d_1}^{\text{tree}} \\
\hat{O}_{d_2}^{\overline{\text{MS}}} &= \left[1 - \frac{g_0^2}{16\pi^2} C_F \left(\frac{7}{6} \log a^2 \mu^2 - \frac{35}{18} + \frac{1}{2}(1 - \alpha) \right) \right] O_{d_2}^{\text{tree}} \\
\hat{O}_{d_3}^{\overline{\text{MS}}} &= \left[1 - \frac{g_0^2}{16\pi^2} C_F \left(\frac{35}{18} \log a^2 \mu^2 - \frac{92}{27} + \frac{5}{6}(1 - \alpha) \right) \right] O_{d_3}^{\text{tree}} \\
\hat{O}_{t_1}^{\overline{\text{MS}}} &= \left[1 - \frac{g_0^2}{16\pi^2} C_F \left(\log a^2 \mu^2 - 1 + (1 - \alpha) \right) \right] O_{t_1}^{\text{tree}} \\
\hat{O}_{t_2}^{\overline{\text{MS}}} &= \left[1 - \frac{g_0^2}{16\pi^2} C_F \left(3 \log a^2 \mu^2 - 5 + \frac{3}{2}(1 - \alpha) \right) \right] O_{t_2}^{\text{tree}} \\
\hat{O}_{t_3}^{\overline{\text{MS}}} &= \left[1 - \frac{g_0^2}{16\pi^2} C_F \left(\frac{13}{3} \log a^2 \mu^2 - \frac{71}{9} + \frac{11}{6}(1 - \alpha) \right) \right] O_{t_3}^{\text{tree}}.
\end{aligned} \quad (37)$$

The connection of overlap lattice fermions with the continuum $\overline{\text{MS}}$ is then given by the gauge-invariant factors

$$\begin{aligned}
\widehat{O}_{v_4,d}^{\overline{\text{MS}}} &= \left[1 - \frac{g_0^2}{16\pi^2} C_F \left(\frac{157}{30} \log a^2 \mu^2 - 73.27869 \right) \right] O_{v_4,d}^{\text{lat (overlap)}} \\
\widehat{O}_{a_4,d}^{\overline{\text{MS}}} &= \left[1 - \frac{g_0^2}{16\pi^2} C_F \left(\frac{157}{30} \log a^2 \mu^2 - 73.27869 \right) \right] O_{a_4,d}^{\text{lat (overlap)}} \\
\widehat{O}_{v_4,e}^{\overline{\text{MS}}} &= \left[1 - \frac{g_0^2}{16\pi^2} C_F \left(\frac{157}{30} \log a^2 \mu^2 - 75.48699 \right) \right] O_{v_4,e}^{\text{lat (overlap)}} \\
\widehat{O}_{a_4,e}^{\overline{\text{MS}}} &= \left[1 - \frac{g_0^2}{16\pi^2} C_F \left(\frac{157}{30} \log a^2 \mu^2 - 75.48699 \right) \right] O_{a_4,e}^{\text{lat (overlap)}} \\
\widehat{O}_{d_1}^{\overline{\text{MS}}} &= \left[1 + \frac{g_0^2}{16\pi^2} C_F \cdot 41.20842 \right] O_{d_1}^{\text{lat (overlap)}} \\
\widehat{O}_{d_2}^{\overline{\text{MS}}} &= \left[1 - \frac{g_0^2}{16\pi^2} C_F \left(\frac{7}{6} \log a^2 \mu^2 - 56.63044 \right) \right] O_{d_2}^{\text{lat (overlap)}} \\
\widehat{O}_{d_3}^{\overline{\text{MS}}} &= \left[1 - \frac{g_0^2}{16\pi^2} C_F \left(\frac{35}{18} \log a^2 \mu^2 - 69.80979 \right) \right] O_{d_3}^{\text{lat (overlap)}} \\
\widehat{O}_{t_1}^{\overline{\text{MS}}} &= \left[1 - \frac{g_0^2}{16\pi^2} C_F \left(\log a^2 \mu^2 - 32.27626 \right) \right] O_{t_1}^{\text{lat (overlap)}} \\
\widehat{O}_{t_2}^{\overline{\text{MS}}} &= \left[1 - \frac{g_0^2}{16\pi^2} C_F \left(3 \log a^2 \mu^2 - 48.73932 \right) \right] O_{t_2}^{\text{lat (overlap)}} \\
\widehat{O}_{t_3}^{\overline{\text{MS}}} &= \left[1 - \frac{g_0^2}{16\pi^2} C_F \left(\frac{13}{3} \log a^2 \mu^2 - 61.42612 \right) \right] O_{t_3}^{\text{lat (overlap)}}.
\end{aligned} \tag{38}$$

For $\beta = 6.0$, $\mu = 1/a$ and $N_c = 3$ one has

$$\begin{aligned}
\widehat{O}_{v_4,d}^{\overline{\text{MS}}} &= 1.61872 O_{v_4,d}^{\text{lat (overlap)}} = 1.19722 O_{v_4,d}^{\text{lat (Wilson)}} \\
\widehat{O}_{a_4,d}^{\overline{\text{MS}}} &= 1.61872 O_{a_4,d}^{\text{lat (overlap)}} = 1.20040 O_{a_4,d}^{\text{lat (Wilson)}} \\
\widehat{O}_{v_4,e}^{\overline{\text{MS}}} &= 1.63737 O_{v_4,e}^{\text{lat (overlap)}} = 1.21534 O_{v_4,e}^{\text{lat (Wilson)}} \\
\widehat{O}_{a_4,e}^{\overline{\text{MS}}} &= 1.63737 O_{a_4,e}^{\text{lat (overlap)}} = 1.21944 O_{a_4,e}^{\text{lat (Wilson)}} \\
\widehat{O}_{d_1}^{\overline{\text{MS}}} &= 1.34794 O_{d_1}^{\text{lat (overlap)}} \\
\widehat{O}_{d_2}^{\overline{\text{MS}}} &= 1.47816 O_{d_2}^{\text{lat (overlap)}} \\
\widehat{O}_{d_3}^{\overline{\text{MS}}} &= 1.58943 O_{d_3}^{\text{lat (overlap)}} \\
\widehat{O}_{t_1}^{\overline{\text{MS}}} &= 1.27252 O_{t_1}^{\text{lat (overlap)}} = 0.85631 O_{t_1}^{\text{lat (Wilson)}} \\
\widehat{O}_{t_2}^{\overline{\text{MS}}} &= 1.41153 O_{t_2}^{\text{lat (overlap)}} = 0.99559 O_{t_2}^{\text{lat (Wilson)}} \\
\widehat{O}_{t_3}^{\overline{\text{MS}}} &= 1.51865 O_{t_3}^{\text{lat (overlap)}} = 1.10021 O_{t_3}^{\text{lat (Wilson)}},
\end{aligned} \tag{39}$$

where we have also shown the corresponding Wilson results (see Eq. (42)). We remind that, although when $\mu = 1/a$ the logarithms disappear from the renormalization factors, for a general μ they are still present but they cancel then against the corresponding logarithms in the Wilson coefficients, as the moments Eq. (6) have to be independent of the renormalization scale (and all the scale dependency is in the logarithms).

The renormalization constants for overlap fermions reported here look in general large, especially when compared to the corresponding Wilson results, as shown in Eq. (39). However, if one looks at the overlap results for the proper diagrams (see for example Appendix B), one can notice that they are not so much different from Wilson fermions. In general, the biggest contribution to the renormalization constants comes from the operator tadpoles, but as they are exactly the same for overlap and Wilson fermions, it is not in these diagrams that the difference can be found. One instead has to look at the quark self-energy (see Appendix A). In the Feynman gauge, the leg self-energy in the overlap (for $\rho = 1$) is -37.63063 , while for Wilson fermions is $+11.85240$; their difference is -49.48303 , and it is remarkable how close this number comes to the differences between the complete finite contributions B_O (defined in Eqs. (29) and (30)) for the two kinds of fermions, Eq. (38) vs. Eq. (42). If one would consider the overlap for $\rho = 1.9$, the difference between the self-energies would go from -49.48303 down to -26.80898 ; however, the quark propagator becomes singular for $\rho = 2$, so simulations would likely be more expensive when approaching this value of ρ .

5.2 Wilson fermions

The 1-loop contributions of the proper diagrams are in the Wilson case

$$\begin{aligned}
O_{v_4,d}^{\text{proper}} &= \frac{g_0^2}{16\pi^2} C_F \left[\left(\frac{127}{30} + (1 - \alpha) \right) \log a^2 p^2 \right. \\
&\quad \left. - 8.359667 - (1 - \alpha) 7.553824 + T_{v_4,d} \right] O_{v_4,d}^{\text{tree}}, \\
O_{a_4,d}^{\text{proper}} &= \frac{g_0^2}{16\pi^2} C_F \left[\left(\frac{127}{30} + (1 - \alpha) \right) \log a^2 p^2 \right. \\
&\quad \left. - 8.736011 - (1 - \alpha) 7.553824 + T_{a_4,d} \right] O_{a_4,d}^{\text{tree}}, \\
O_{v_4,e}^{\text{proper}} &= \frac{g_0^2}{16\pi^2} C_F \left[\left(\frac{127}{30} + (1 - \alpha) \right) \log a^2 p^2 \right. \\
&\quad \left. - 6.684639 - (1 - \alpha) 8.024764 + T_{v_4,e} \right] O_{v_4,e}^{\text{tree}},
\end{aligned}$$

$$\begin{aligned}
O_{a_4,e}^{\text{proper}} &= \frac{g_0^2}{16\pi^2} C_F \left[\left(\frac{127}{30} + (1-\alpha) \right) \log a^2 p^2 \right. \\
&\quad \left. -7.171210 - (1-\alpha) 8.024764 + T_{a_4,e} \right] O_{a_4,e}^{\text{tree}}, \\
O_{d_1}^{\text{proper}} &= \frac{g_0^2}{16\pi^2} C_F \left[-\alpha \log a^2 p^2 + 0.745643 - (1-\alpha) 7.850272 + T_{d_1} \right] O_{d_1}^{\text{tree}} \\
&\quad + 16.243762 \frac{i}{a} \frac{g_0^2}{16\pi^2} C_F \bar{\psi} \sigma_{41} \gamma_5 \psi \\
O_{d_2}^{\text{proper}} &= \frac{g_0^2}{16\pi^2} C_F \left[\left(\frac{1}{6} + (1-\alpha) \right) \log a^2 p^2 \right. \\
&\quad \left. -3.063751 - (1-\alpha) 8.369693 + T_{d_2} \right] O_{d_2}^{\text{tree}} \\
&\quad + 4.265680 \frac{1}{a} \frac{g_0^2}{16\pi^2} C_F \left(\bar{\psi} \gamma_4 \gamma_5 \gamma_{\{1} D_{2\}} \psi - \bar{\psi} \gamma_1 \gamma_5 \gamma_{\{4} D_{2\}} \psi \right) \\
O_{d_3}^{\text{proper}} &= \frac{g_0^2}{16\pi^2} C_F \left[\left(\frac{17}{18} + (1-\alpha) \right) \log a^2 p^2 \right. \\
&\quad \left. -4.902360 - (1-\alpha) 8.553824 + T_{d_3} \right] O_{d_3}^{\text{tree}} \\
&\quad + 2.881820 \frac{1}{a} \frac{g_0^2}{16\pi^2} C_F \left(\bar{\psi} \gamma_4 \gamma_5 \gamma_{\{1} D_2 D_{3\}} \psi - \bar{\psi} \gamma_1 \gamma_5 \gamma_{\{4} D_2 D_{3\}} \psi \right) \\
O_{t_1}^{\text{proper}} &= \frac{g_0^2}{16\pi^2} C_F \left[(1-\alpha) \log a^2 p^2 \right. \\
&\quad \left. +4.165675 - (1-\alpha) 3.792010 + T_{t_1} \right] O_{t_1}^{\text{tree}} \\
O_{t_2}^{\text{proper}} &= \frac{g_0^2}{16\pi^2} C_F \left[\left(2 + (1-\alpha) \right) \log a^2 p^2 \right. \\
&\quad \left. -4.096894 - (1-\alpha) 6.350272 + T_{t_2} \right] O_{t_2}^{\text{tree}} \\
O_{t_3}^{\text{proper}} &= \frac{g_0^2}{16\pi^2} C_F \left[\left(\frac{10}{3} + (1-\alpha) \right) \log a^2 p^2 \right. \\
&\quad \left. -7.143946 - (1-\alpha) 7.036360 + T_{t_3} \right] O_{t_3}^{\text{tree}},
\end{aligned} \tag{40}$$

where $\sigma_{\mu\nu} = \frac{i}{2}[\gamma_\mu, \gamma_\nu]$.

The operator tadpoles are the same as in the overlap case (see Table 2). Adding the quark self-energy (appendix A), the complete renormalization factors are then

$$\begin{aligned}
\widehat{O}_{v_4,d}^{\text{Wilson}} &= \left[1 - \frac{g_0^2}{16\pi^2} C_F \left(\frac{157}{30} \log a^2 \mu^2 - 33.206413 + \frac{11}{6}(1-\alpha) \right) \right] O_{v_4,d}^{\text{tree}} \\
\widehat{O}_{a_4,d}^{\text{Wilson}} &= \left[1 - \frac{g_0^2}{16\pi^2} C_F \left(\frac{157}{30} \log a^2 \mu^2 - 33.582757 + \frac{11}{6}(1-\alpha) \right) \right] O_{a_4,d}^{\text{tree}} \\
\widehat{O}_{v_4,e}^{\text{Wilson}} &= \left[1 - \frac{g_0^2}{16\pi^2} C_F \left(\frac{157}{30} \log a^2 \mu^2 - 35.351922 + \frac{11}{6}(1-\alpha) \right) \right] O_{v_4,e}^{\text{tree}} \\
\widehat{O}_{a_4,e}^{\text{Wilson}} &= \left[1 - \frac{g_0^2}{16\pi^2} C_F \left(\frac{157}{30} \log a^2 \mu^2 - 35.838493 + \frac{11}{6}(1-\alpha) \right) \right] O_{a_4,e}^{\text{tree}} \\
\widehat{O}_{d_1}^{\text{Wilson}} &= \left[1 - \frac{g_0^2}{16\pi^2} C_F \cdot 0.364997 \right] O_{d_1}^{\text{tree}} \\
&\quad - 16.243762 \frac{i}{a} \frac{g_0^2}{16\pi^2} C_F \bar{\psi} \sigma_{41} \gamma_5 \psi \\
\widehat{O}_{d_2}^{\text{Wilson}} &= \left[1 - \frac{g_0^2}{16\pi^2} C_F \left(\frac{7}{6} \log a^2 \mu^2 - 15.677447 + \frac{1}{2}(1-\alpha) \right) \right] O_{d_2}^{\text{tree}} \\
&\quad - 4.265680 \frac{1}{a} \frac{g_0^2}{16\pi^2} C_F (\bar{\psi} \gamma_4 \gamma_5 \gamma_{\{1} D_2 \} \psi - \bar{\psi} \gamma_1 \gamma_5 \gamma_{\{4} D_2 \} \psi) \\
\widehat{O}_{d_3}^{\text{Wilson}} &= \left[1 - \frac{g_0^2}{16\pi^2} C_F \left(\frac{35}{18} \log a^2 \mu^2 - 29.749107 + \frac{5}{6}(1-\alpha) \right) \right] O_{d_3}^{\text{tree}} \\
&\quad - 2.881820 \frac{1}{a} \frac{g_0^2}{16\pi^2} C_F (\bar{\psi} \gamma_4 \gamma_5 \gamma_{\{1} D_2 D_3 \} \psi - \bar{\psi} \gamma_1 \gamma_5 \gamma_{\{4} D_2 D_3 \} \psi) \\
\widehat{O}_{t_1}^{\text{Wilson}} &= \left[1 - \frac{g_0^2}{16\pi^2} C_F \left(\log a^2 \mu^2 + 16.018079 + (1-\alpha) \right) \right] O_{t_1}^{\text{tree}} \\
\widehat{O}_{t_2}^{\text{Wilson}} &= \left[1 - \frac{g_0^2}{16\pi^2} C_F \left(3 \log a^2 \mu^2 - 4.477540 + \frac{3}{2}(1-\alpha) \right) \right] O_{t_2}^{\text{tree}} \\
\widehat{O}_{t_3}^{\text{Wilson}} &= \left[1 - \frac{g_0^2}{16\pi^2} C_F \left(\frac{13}{3} \log a^2 \mu^2 - 19.757642 + \frac{11}{6}(1-\alpha) \right) \right] O_{t_3}^{\text{tree}}.
\end{aligned} \tag{41}$$

We can see that for Wilson fermions the operators O_{d_1} , O_{d_2} and O_{d_3} are not multiplicatively renormalized. Each of them mixes with an operator which is one dimension lower [17], and the corresponding mixing coefficients, which seem to be gauge-invariant, are proportional to r/a . Thus, these mixings would be zero for naive fermions, and they are akin to the Σ_0 term in the Wilson quark self-energy, which is responsible for the additive renormalization of quark masses when they are not anymore protected by chirality. In fact, the lower-dimensional operators above are all mass terms of the form (19) coming from the OPE expansions in DIS. All this hints to a connection with chirality in the mixings of the O_{d_n} operators too, and we have indeed shown in Eq. (35) that in the calculations done with overlap fermions, where chirality is conserved, there is no trace of this kind of terms and these operators are then multiplicatively renormalized.

We can also notice from the Wilson results above that another consequence of

the breaking of chiral invariance is that the renormalization constants of $O_{v_4,d}$ and $O_{a_4,d}$ are not equal, and the same happens for $O_{v_4,e}$ and $O_{a_4,e}$.

The perturbative calculations with Wilson fermions of the renormalization constants for the operators $O_{v_4,d}$, $O_{a_4,d}$, $O_{v_4,e}$, O_{d_2} and O_{t_1} have been already done in the past in Feynman gauge. We agree with the results for $O_{v_4,d}$ and $O_{a_4,d}$ in Ref. [25], but we find discrepancies with the renormalization of $O_{v_4,e}$ in Ref. [17]⁴. We agree also with the results for O_{d_2} in Ref. [17] and for O_{t_1} in Ref. [22].

The connection of Wilson fermions with the continuum $\overline{\text{MS}}$ is given by

$$\begin{aligned}
\widehat{O}_{v_4,d}^{\overline{\text{MS}}} &= \left[1 - \frac{g_0^2}{16\pi^2} C_F \left(\frac{157}{30} \log a^2 \mu^2 - 23.357525 \right) \right] O_{v_4,d}^{\text{lat (Wilson)}} \\
\widehat{O}_{a_4,d}^{\overline{\text{MS}}} &= \left[1 - \frac{g_0^2}{16\pi^2} C_F \left(\frac{157}{30} \log a^2 \mu^2 - 23.733869 \right) \right] O_{a_4,d}^{\text{lat (Wilson)}} \\
\widehat{O}_{v_4,e}^{\overline{\text{MS}}} &= \left[1 - \frac{g_0^2}{16\pi^2} C_F \left(\frac{157}{30} \log a^2 \mu^2 - 25.503033 \right) \right] O_{v_4,e}^{\text{lat (Wilson)}} \\
\widehat{O}_{a_4,e}^{\overline{\text{MS}}} &= \left[1 - \frac{g_0^2}{16\pi^2} C_F \left(\frac{157}{30} \log a^2 \mu^2 - 25.989604 \right) \right] O_{a_4,e}^{\text{lat (Wilson)}} \\
\widehat{O}_{t_1}^{\overline{\text{MS}}} &= \left[1 - \frac{g_0^2}{16\pi^2} C_F \left(\log a^2 \mu^2 + 17.018079 \right) \right] O_{t_1}^{\text{lat (Wilson)}} \\
\widehat{O}_{t_2}^{\overline{\text{MS}}} &= \left[1 - \frac{g_0^2}{16\pi^2} C_F \left(3 \log a^2 \mu^2 + 0.522460 \right) \right] O_{t_2}^{\text{lat (Wilson)}} \\
\widehat{O}_{t_3}^{\overline{\text{MS}}} &= \left[1 - \frac{g_0^2}{16\pi^2} C_F \left(\frac{13}{3} \log a^2 \mu^2 - 11.868753 \right) \right] O_{t_3}^{\text{lat (Wilson)}},
\end{aligned} \tag{42}$$

and the numbers for $\beta = 6.0$, $\mu = 1/a$ and $N_c = 3$ are given in Eq. (39). We have not included here O_{d_1} , O_{d_2} and O_{d_3} , as their renormalization involves mixing coefficients that diverge in the limit of zero lattice spacing, and as such it is of no use to compute the connection to $\overline{\text{MS}}$ for these operators in perturbation theory with Wilson fermions.

⁴ In this case we do not even agree on the results for the individual proper diagrams, which are given in Table 5 of Ref. [17]. In that Table, the operator tadpole is given the value that would be appropriate for $O_{v_4,d}$, but this cannot be true for $O_{v_4,e}$, since there are additional Wick contractions between the A_μ s originating from the equal indices.

6 Conclusions

Overlap fermions are one of the most promising formulations for putting chiral fermions on the lattice and for studying long-standing problems linked with chirality. In this paper we have computed the renormalization constants of the lowest moments of various structure functions which give a complete description of the quark momentum and spin at leading twist. We have computed these constants also with Wilson fermions, since the renormalization of many of these operators had never before been computed on the lattice. Chiral symmetry plays an important role in the structure of the strong radiative corrections. In particular, the overlap is the only case in which it has yet been demonstrated that all the operators we have considered are multiplicatively renormalized.

The numbers presented here are also valid in the unquenched case if one deals with flavor non-singlet quark operators, which do not mix with gluon operators and for which internal quark loops never have the chance to come to play at 1-loop level. However, the numbers for the transversity operators can be considered unquenched also for flavor singlet quark operators, since there are no gluon operators with the same quantum numbers.

We remind again that all the renormalization constants presented in this paper are already fully $O(a)$ improved in the overlap case. In the Wilson case removing all order a effects would instead involve a great amount of additional calculations.

With overlap fermions 1-loop corrections are substantially larger than for Wilson fermions, with the primary contribution arising from quark self-energies. This is an important physical effect that should be understood, and may ultimately suggest an appropriate form of resummation or tadpole improvement.

Acknowledgment

I would like to thank John W. Negele for critically reading the manuscript and discussion. This work has been supported in part by the U.S. Department of Energy (DOE) under cooperative research agreement DE-FC02-94ER40818. Both the FORM and Fortran computations have been done at MIT on a few Pentium III PCs running on Linux.

ρ	non-tadpole self-energy	leg tadpole	total self-energy
0.2	-27.511695 +11.911596 ξ	-213.087934 -7.119586 ξ	-240.599629 +4.792010 ξ
0.3	-23.687573 +11.098129 ξ	-131.723110 -6.306119 ξ	-155.410693 +4.792010 ξ
0.4	-21.172454 +10.520210 ξ	-91.817537 -5.728200 ξ	-112.989991 +4.792010 ξ
0.5	-19.337313 +10.071356 ξ	-68.315503 -5.279346 ξ	-87.652816 +4.792010 ξ
0.6	-17.912921 +9.704142 ξ	-52.931363 -4.912132 ξ	-70.844284 +4.792010 ξ
0.7	-16.760616 +9.393275 ξ	-42.140608 -4.601265 ξ	-58.901224 +4.792010 ξ
0.8	-15.800204 +9.123666 ξ	-34.193597 -4.331656 ξ	-49.993801 +4.792010 ξ
0.9	-14.981431 +8.885590 ξ	-28.125054 -4.093580 ξ	-43.106485 +4.792010 ξ
1.0	-14.270881 +8.672419 ξ	-23.359746 -3.880409 ξ	-37.630627 +4.792010 ξ
1.1	-13.645294 +8.479438 ξ	-19.534056 -3.687428 ξ	-33.179350 +4.792010 ξ
1.2	-13.087876 +8.303183 ξ	-16.407174 -3.511173 ξ	-29.495050 +4.792010 ξ
1.3	-12.586126 +8.141044 ξ	-13.813486 -3.349034 ξ	-26.399612 +4.792010 ξ
1.4	-12.130497 +7.991018 ξ	-11.635482 -3.199008 ξ	-23.765979 +4.792010 ξ
1.5	-11.713524 +7.851554 ξ	-9.787582 -3.059544 ξ	-21.501106 +4.792010 ξ
1.6	-11.329238 +7.721442 ξ	-8.206069 -2.929432 ξ	-19.535307 +4.792010 ξ
1.7	-10.972744 +7.599750 ξ	-6.842630 -2.807740 ξ	-17.815374 +4.792010 ξ
1.8	-10.639905 +7.485778 ξ	-5.660084 -2.693768 ξ	-16.299989 +4.792010 ξ
1.9	-10.327042 +7.379023 ξ	-4.629539 -2.587013 ξ	-14.956581 +4.792010 ξ

Table A.1

Results for the quark self-energy with overlap fermions, where we have used the abbreviation $\xi = 1 - \alpha$. The first column (non-tadpole self-energy) refers to diagram e (or f) in Fig. 1, and the second column (leg tadpole) refers to diagram g (or h).

A Quark self-energy

In this appendix we report the results of 1-loop calculations regarding the contribution proportional to $i\not{p}$ of the quark self-energy, also known as Σ_1 . This corresponds to the diagrams e (or f) and g (or h) in Fig. 1, and is necessary for the calculation of the renormalization constants of the operators considered in this work.

For overlap fermions we have that the total self-energy is given by

$$\Sigma_1^{\text{overlap}} = \frac{g_0^2}{16\pi^2} C_F \left[\alpha \log a^2 p^2 + S^{\alpha=1} + (1 - \alpha) 4.792010 \right], \quad (\text{A.1})$$

where the Feynman-gauge finite results $S^{\alpha=1}$ are given in the last column of Table A.1 (in which we have used the abbreviation $\xi = 1 - \alpha$), which also contains the results of the individual diagrams. For the total self-energy (but not for the individual diagrams) the finite part proportional to $(1 - \alpha)$ is independent of the ρ parameter, and even of the fermion action used. In fact this number comes from integrals which have only gluonic propagators, and is given by $F_0 - \gamma_E + 1 = 4.792009568973 \dots$ [9].

In the Wilson case, the value of the leg self-energy (including the tadpole) is

$$\Sigma_1^{\text{Wilson}} = \frac{g_0^2}{16\pi^2} C_F \left[\alpha \log a^2 p^2 + 11.852404 + (1 - \alpha) 4.792010 \right]. \quad (\text{A.2})$$

The result for the individual diagrams is the following: for diagram e (or f) is

$$\frac{g_0^2}{16\pi^2} C_F \left[\alpha \log a^2 p^2 - 0.380646 + (1 - \alpha) 7.850272 \right], \quad (\text{A.3})$$

while the leg tadpole, i.e. diagram g (or h), is

$$g_0^2 C_F \left[\frac{1}{2} Z_0 - (1 - \alpha) \frac{1}{8} Z_0 \right] = \frac{g_0^2}{16\pi^2} C_F \left[12.233050 - (1 - \alpha) 3.058262 \right], \quad (\text{A.4})$$

where $Z_0 = 0.154933390231 \dots$.

B Results of the individual diagrams

In this appendix we give the results for the finite parts of the proper diagrams: the vertex (diagram a in Fig. 1), the sails (diagrams b plus c) and the operator tadpole (diagram d). We have used the abbreviation $\xi = 1 - \alpha$. Table B.1 refers to overlap fermions (for $\rho = 1$) and Table B.2 to Wilson fermions. For the latter, Table B.3 also reports the numbers giving the mixing with the lower dimensional operators.

Note that the sum of the $(1 - \alpha)$ parts of vertex and sails is independent of the fermion action used, and in general this is also true for the individual

	vertex (diagram a)	sails (diagrams b + c)	op. tadpole (diagram d)
$O_{v4,d}$	0.70281 -0.53019 ξ	-9.50061 -7.02363 ξ	-36.69915 +4.59515 ξ
$O_{a4,d}$	0.70281 -0.53019 ξ	-9.50061 -7.02363 ξ	-36.69915 +4.59515 ξ
$O_{v4,e}$	0.61867 -0.05926 ξ	-7.80424 -7.96551 ξ	-40.51969 +5.06609 ξ
$O_{a4,e}$	0.61867 -0.05926 ξ	-7.80424 -7.96551 ξ	-40.51969 +5.06609 ξ
O_{d1}	2.81906 -0.65840 ξ	5.83620 -7.19187 ξ	-12.23305 +3.05826 ξ
O_{d2}	1.15709 -0.49753 ξ	2.36476 -7.87216 ξ	-24.46610 +4.07768 ξ
O_{d3}	0.64918 -0.45310 ξ	0.46340 -8.10072 ξ	-36.69915 +4.59515 ξ
O_{t1}	4.35437 -3.79201 ξ	0	0
O_{t2}	1.46711 -1.23375 ξ	-5.34275 -5.11652 ξ	-12.23305 +3.05826 ξ
O_{t3}	0.68662 -0.54766 ξ	-7.90490 -6.48870 ξ	-24.46610 +4.07768 ξ

Table B.1

Results of the proper diagrams for overlap fermions, where we have used the abbreviation $\xi = 1 - \alpha$.

	vertex (diagram a)	sails (diagrams b + c)	op. tadpole (diagram d)
$O_{v4,d}$	0.842048 -0.530195 ξ	-9.201715 -7.023629 ξ	-36.699150 +4.595148 ξ
$O_{a4,d}$	0.465704 -0.530195 ξ	-9.201715 -7.023629 ξ	-36.699150 +4.595148 ξ
$O_{v4,e}$	0.842455 -0.059255 ξ	-7.527094 -7.965509 ξ	-40.519687 +5.066088 ξ
$O_{a4,e}$	0.355884 -0.059255 ξ	-7.527094 -7.965509 ξ	-40.519687 +5.066088 ξ
O_{d1}	2.590817 -0.812814 ξ	-1.845174 -7.037458 ξ	-12.233050 +3.058263 ξ
O_{d2}	0.988791 -0.585340 ξ	-4.052542 -7.784353 ξ	-24.466100 +4.077683 ξ
O_{d3}	0.536160 -0.521292 ξ	-5.438520 -8.032532 ξ	-36.699150 +4.595148 ξ
O_{t1}	4.165675 -3.792010 ξ	0	0
O_{t2}	0.980373 -1.233747 ξ	-5.077267 -5.116525 ξ	-12.233050 +3.058263 ξ
O_{t3}	0.465618 -0.547660 ξ	-7.609564 -6.488700 ξ	-24.466100 +4.077683 ξ

Table B.2

Results of the proper diagrams for Wilson fermions, where we have used the abbreviation $\xi = 1 - \alpha$.

	vertex (diagram a)	sails (diagrams b + c)	op. tadpole (diagram d)
O_{d1}	1.508200	14.735561	0
O_{d2}	0.180285	4.085395	0
O_{d3}	0.073704	2.808116	0

Table B.3

Results for the mixing with the lower-dimensional operators for Wilson fermions.

diagrams. An exception to this are the O_{d_n} operators and the quark self-energy, and these are also the same cases for which with Wilson fermions there is a 1-loop mixing with a $1/a$ divergent coefficient, while with overlap fermions such mixings are forbidden by chiral symmetry.

References

- [1] R. Narayanan and H. Neuberger, Nucl. Phys. **B443** (1995) 305;
R. Narayanan and H. Neuberger, Phys. Lett. **B302** (1993) 62.
- [2] H. Neuberger, Phys. Lett. **B417** (1998) 141;
H. Neuberger, Phys. Lett. **B427** (1998) 353.
- [3] P. H. Ginsparg and K. G. Wilson, Phys. Rev. **D25** (1982) 2649.
- [4] M. Lüscher, Phys. Lett. **B428** (1998) 342.
- [5] P. Hernández, K. Jansen and M. Lüscher, Nucl. Phys. **B552** (1999) 363.
- [6] H. Neuberger, Phys. Rev. **D57** (1998) 5417;
H. Neuberger, Phys. Rev. Lett. **81** (1998) 4060;
H. Neuberger, Nucl. Phys. **B** (Proc. Suppl.) **83** (2000) 813;
R. Narayanan and H. Neuberger, Phys. Rev. **D62** (2000) 074504;
R. G. Edwards, U. M. Heller and R. Narayanan, Nucl. Phys. **B540** (1999) 457;
R. G. Edwards, U. M. Heller and R. Narayanan, Phys. Rev. **D59** (1999) 094510;
A. Bode, U. M. Heller, R. G. Edwards and R. Narayanan, “First experiences with HMC for dynamical overlap fermions”, hep-lat/9912043;
P. Hernández, K. Jansen and L. Lellouch, “A numerical treatment of Neuberger’s lattice Dirac operator”, hep-lat/0001008.
- [7] L. Giusti, C. Hoelbling and C. Rebbi, in preparation;
L. Giusti, C. Hoelbling and C. Rebbi, to appear in the Proceedings of the Lattice 2000 International Symposium, to be published in Nucl. Phys. **B** (Proc. Suppl.).

- [8] S. J. Dong, F. X. Lee, K. F. Liu and J. B. Zhang, “Chiral Symmetry, Quark Mass, and Scaling of the Overlap Fermions”, hep-lat/0006004;
S. J. Dong, F. X. Lee, K. F. Liu and J. B. Zhang, to appear in the Proceedings of the Lattice 2000 International Symposium, to be published in Nucl. Phys. **B** (Proc. Suppl.).
- [9] S. Capitani and L. Giusti, “Perturbative Renormalization of Weak-Hamiltonian Four-Fermion Operators with Overlap Fermions”, hep-lat/0007011, to be published in Phys. Rev. **D**.
- [10] P. Hernández, K. Jansen and M. Lüscher, “A note on the practical feasibility of domain-wall fermions”, hep-lat/0007015.
- [11] S. Capitani, “Perturbative Renormalization of the First Two Moments of Non-Singlet Quark Distributions with Overlap Fermions”, hep-lat/0005008.
- [12] J. Ralston and D. E. Soper, Nucl. Phys. **B152** (1979) 109;
R. L. Jaffe and X. Ji, Phys. Rev. Lett. **67** (1991) 552;
R. L. Jaffe and X. Ji, Nucl. Phys. **B375** (1992) 527.
- [13] X. Artru and M. Mekhfi, Z. Phys. **C45** (1990) 669;
X. Artru and M. Mekhfi, Nucl. Phys. **A532** (1991) 351.
- [14] X. Ji and C. Chou, Phys. Rev. **D42** (1990) 3637;
R. L. Jaffe and X. Ji, Phys. Rev. **D43** (1991) 724.
- [15] S. Capitani and G. C. Rossi, Nucl. Phys. **B433** (1995) 351.
- [16] G. Beccarini, M. Bianchi, S. Capitani and G. C. Rossi, Nucl. Phys. **B456** (1995) 271.
- [17] M. Göckeler et al., Nucl. Phys. **B472** (1996) 309;
M. Göckeler et al., Phys. Rev. **D53** (1996) 2317.
- [18] M. Göckeler et al., Nucl. Phys. **B** (Proc. Suppl.) **53** (1997) 81;
M. Göckeler et al., Nucl. Phys. **B** (Proc. Suppl.) **53** (1997) 896.
- [19] S. Capitani et al., “Local bilinear operators on the lattice and their perturbative renormalisation including $O(a)$ effects”, hep-lat/9711007, in: “Deep Inelastic Scattering off Polarized Targets: Theory Meets Experiment”, Proceedings of the SPIN97 Topical Workshop, J. Blümlein, A. De Roeck, T. Gehrmann and W.-D. Nowak eds. (DESY, 1997), p. 266;
S. Capitani et al., Nucl. Phys. **B** (Proc. Suppl.) **63** (1998) 874.
- [20] A. Bucarelli, F. Palombi, R. Petronzio and A. Shindler, Nucl. Phys. **B552** (1999) 379;
M. Guagnelli, K. Jansen and R. Petronzio, Nucl. Phys. **B542** (1999) 395;
M. Guagnelli, K. Jansen and R. Petronzio, Phys. Lett. **B459** (1999) 594.
- [21] A. V. Manohar, “An Introduction to Spin Dependent Deep Inelastic Scattering”, Lectures given at Lake Louise Winter Inst., Lake Louise, Canada, 1992; hep-ph/9204208.

- [22] S. Capitani, M. Göckeler, R. Horsley, H. Perlt, P. E. L. Rakow, A. Schiller and G. Schierholz, “Renormalisation and off-shell Improvement in Lattice Perturbation Theory”, hep-lat/0007004.
- [23] S. Capitani, M. Göckeler, R. Horsley, P. E. L. Rakow and G. Schierholz, Phys. Lett. **B468** (1999) 150;
S. Capitani, M. Göckeler, R. Horsley, P. E. L. Rakow and G. Schierholz, Nucl. Phys. **B** (Proc. Suppl.) **83-84** (2000) 893.
- [24] C. Alexandrou, E. Follana, H. Panagopoulos and E. Vicari, Nucl. Phys. **B580** (2000) 394.
- [25] R. C. Brower, S. Huang, J. W. Negele, A. Pochinsky and B. Schreiber, Nucl. Phys. **B** (Proc. Suppl.) **53** (1997) 318.